PNAS

Supporting Information for

Externalized histones fuel pulmonary fibrosis via a platelet-macrophage circuit of TGFβ1 and IL-27

Dennis R. Riehl, Arjun Sharma, Julian Roewe, Florian Murke, Clemens Ruppert, Sabine A. Eming, Tobias Bopp, Hartmut Kleinert, Markus P. Radsak, Giuseppe Colucci, Saravanan Subramaniam, Christoph Reinhardt, Bernd Giebel, Immo Prinz, Andreas Guenther, Dennis Strand, Matthias Gunzer, Ari Waisman, Peter A. Ward, Wolfram Ruf, Katrin Schäfer, Markus Bosmann

Corresponding Author: Markus Bosmann, Associate Professor of Medicine, Pathology & Laboratory Medicine, Pulmonary Center, Department of Medicine, Boston University School of Medicine, Boston, Massachusetts, 02118, USA, Phone: +1-617-358-1225, FAX: +1-617-638-5227. E-mail: mbosmann@bu.edu

This PDF file includes:

Supporting Information Text

Extended Methods

Mice

Mice of the strains C57BL/6J, IL-27RA$^{-/-}$ (B6N.129P2-Il27ratm1Mak/J), $^{\Delta Mye}$TbRII (Tgfbr2^{tm1Roes} x Lyz2$^{tm1(cre)Ifo}$), $^{\Delta Plt}$TGFβ1 (C57BL/6-Tg(Pf4-cre)Q3Rsko/J x Tgfb1$^{tm2.1Doe/}$J), H2B-eGFP (B6.Cg-Tg(HIST1H2BB/EGFP)1Pa/J), TTP$^{-/-}$ (1), IL-17A$^{-/-}$IL-17F$^{-/-}$ (B6.Cg-Il17a/Il17f$^{tm1.1Impr}$Thy1^{a}/J) , MyD88$^{-/-}$ (B6.129P2(SJL)-Myd88$^{tm1.1Defr}$/J), IL-10$^{-/-}$ (B6.129P2-Il10^{tm1Cgn}/J), TRIF$^{-/-}$ (C57BL/6J-Ticam1^{Lps2}/J), PAD4$^{-/-}$ (B6.Cg-Padi4$^{tm1.2Kmow}$/J), TLR2$^{-/-}$ (B6.129-Tlr2^{tm1Kir}/J) and TLR4$^{-/-}$ (B6.129P2-Tlr4^{tm1Aki}) were bred and/or housed under specific pathogen-free conditions at the animal facilities of the Johannes Gutenberg-University Mainz and Boston University. Mice (8-12 weeks old) on a C57BL/6J background were used for experiments.

Bleomycin-induced Pulmonary Fibrosis

For bleomycin-induced lung fibrosis mice were anesthetized by intra-peritoneal injection of ketamine (100 mg/kg body weight) and xylazin (8 mg/kg body weight) followed by surgical exploration and intra-tracheal application of bleomycin (1 U/kg body weight; Bleomedac®; Medac GmbH, Wedel, Germany) in 40µl NaCl 0.9%. At the end of experiments, mice were euthanized followed by tracheal cannulation for BAL with 1 ml sterile PBS and harvesting of lung tissue. Lavage fluids were centrifuged (300g, 5 min, 4°C) for separation of cells and stored at -80°C until analysis. Lung tissue was stored at -80°C and homogenized (Tissue Lyser II, Qiagen) before further analysis.

Bone Marrow Transplantation

Mice were γ-irradiated (^{137}Cs) with 2x6.5 Gy in a 3 h interval. 5x10^{6} donor bone marrow cells in 200 µl RPMI 1640 (supplemented with 100 units/ml penicillin-streptomycin and 0.1% BSA) were transplanted by tail vein injection into recipient mice. Mice received acidified water (pH 3.0) for 5 weeks. This protocol was validated before for engraftment and ~80% depletion of alveolar macrophages (2).

Macrophages

Primary alveolar macrophages were obtained by multiple BALs (20 x 1 ml PBS, without Ca^{2+}/Mg^{2+}, 0.5 mM EDTA) as described by us before (3). Bone marrow derived macrophages (BMDM) were differentiated from bone marrow cells by 7 day culture with L929 cell-conditioned media, peritoneal elicited macrophages (PEM) were isolated 4 days after thioglycollate (1.5 ml i.p., 2.4% w/v) (4-6). Macrophages were cultured in RPMI 1640 (100 units/ml penicillin-streptomycin plus 0.1% BSA for primary macrophages or 10% FCS for RAW264.7 and MH-S macrophages) at 37°C, 5% CO_2.

MLE-12 Cells

The murine lung epithelial cell line, MLE-12, was cultured in RPMI 1640 supplemented with 2mM L-Glutamine, 2% FCS, 100 U/ml Penicillin/Streptomycin, 10 mM HEPES, 10 nM Hydrocortisone, 10 nM Estradiol, and 1 x Insulin/Transferrin/Selenite (3, 7). For experiments, the cells were transferred to RPMI 1640 medium (w/o phenol red) supplemented with 100 U/ml Penicillin/Streptomycin and 10 mM HEPES.

Lentiviral Transductions

RAW264.7 macrophages ($5x10^4$) were transduced in 300 µl media with an MOI20 of pLKO.1-puro lentiviral particles (TRCN0000089023, TRCN0000089024, SHC002V, MISSION®, Sigma-Aldrich, St. Louis, MO) for shRNA knock-down of SMAD3 or non-target (non-mammalian) shRNA controls. The sequences can be found as Supplementary Table S2. RAW264.7 cells received fresh media on day 2 and were reseeded on day 4 in medium supplemented with 5 µg/ml puromycin (Sigma-Aldrich) for selection of stable transduced clones. After 2 weeks in culture, knock-down efficacy was confirmed (see Supplementary Figure S6D, S6E) and cells were passaged with regular intervals of puromycin treatment.

Platelets

Platelet rich plasma was obtained by centrifuging (180g, 5 min, 20°C). Platelets were pelleted by centrifugation (300g, 5 min, 20°C), washed once in Tyrode's buffer, pH 6.5 (300g, 5 min, 20°C) and resuspended in Tyrode's buffer, pH 7.4 followed by counting (KX-21N Sysmex, Hematology Diagnostics, Kobe, Japan). Aggregation of washed platelets was measured by light transmission (Born aggregometry, APACT 4S PLUS, software v1.21c, DiaSys Greiner, Flacht, Germany) within 10 min at 37°C. Supernatants of $5x10^5$ platelets/well were pH-activated before transfer to 24-well macrophage cultures.

Enzyme linked immunosorbent assays (ELISA)

For the measurement of IL-27p28, IL-10 and TGFβ1 the ELISA kits from R&D Systems, and histone H4 was analyzed using an ELISA kit from Abcam (Waltham, MA). Protocols were used according to manufacturer's instructions. To detect citrullinated histones in cell-free samples (300g, 5 min, 4°C), the ELISA plates were coated with anti-citH3 (Abcam, 4µg/ml) followed by the secondary antibody of the Cell Death Detection ELISA^{PLUS}, v12 kit (Roche; Sigma-Aldrich) (8). Optical densities (405 nm, 450 nm) were measured with an Opsys MR Dynex microplate reader and concentrations calculated with Revelation V G3.2 (Dynex Technologies); or with a Tecan Infinite M Nano plate reader using Magellan software.

Collagen Assay

For collagen I-V measurements, the left lungs were isolated and processed according to the manufacturer's protocol of the SIRCOL^{TM} Collagen Assay (Biocolor, Carrickfergus, UK) with lung digestion for 24 h at 4°C (0.1 mg/ml pepsin in 0.5M acetic acid).

Bead-based protein assays

The quantification of mouse cytokines/chemokines (Bio-Plex Pro^{TM}, BioRad, Hercules, CA) and phosphorylated Thr^{180}/Tyr^{182} p38 MAPK (Bio-Plex Pro^{TM} Cell Signaling Assay, BioRad) was done according to manufacturer's instructions as described before (9). The Luminex-200/BioPlex-200 system (BioRad) with the Bio-Plex Manager 6.1 (BioRad) was utilized for data acquisition.

Flow cytometry

Flow cytometry staining was performed as described before (5). We used either 2 µM Monensin (IL-27p28) or 5 µg/ml Brefeldin A as golgi transport inhibitors for intracellular cytokine detection. For IL-17A/IFNγ staining, the cells were stimulated with anti-CD3/anti-CD28 for 4 h. For detection of extracellular citrullinated histone H3 from NETs, non-permeabilized BALF cells were fixed with 2% paraformaldehyde for 8-10 min and stained with primary rabbit anti-mouse citH3 antibody (1:250, Abcam) followed by secondary AF488-conjugated goat anti-rabbit IgG (1:500, Abcam). All antibodies were used with matched fluorochrome-labeled isotype controls. The entire list of antibodies can be found as Supplementary Table S3. To calculate total cell counts, samples were supplemented with 123count eBeads (eBioscience, San Diego, CA). A BD

Canto II flow cytometer (BD Biosciences, Woburn, MA) and FlowJo 10.0 software were used for data acquisition and analysis.

Imaging Flow Cytometry

Imaging flow cytometry analysis were performed with the ImageStreamX Mark II (Merck, Darmstadt, Germany) using the Inspire data acquisition software (Merck). Samples were stained according to the flow cytometry protocol describe above and were recorded with a 60x magnitude and the lowest flow speed. Data and picture preparation was conducted in the IDEAS software (Merck). After selection of single and focused cells, using predefined building blocks, $Ly6G^{+}citH3^{+}$ cells were defined. Inside this population of interest the NET-forming cells were enriched by gating on events, which harbored a low aspect ratio (morphology mask) and high bright detail intensity (default mask) in the citH3 detecting channel (*SI Appendix*, Fig. S1).

Reverse Transcription PCR

Total RNA was isolated (RNeasy Mini Kit, QIAGEN) from cells or homogenized tissues (TissueLyser, QIAGEN, Hilden, Germany). Concentration of total RNA was measured with a NanoDrop2000c (ThermoFisher Scientific, Waltham, MA). The cDNA was generated with a High-Capacity cDNA Reverse Transcription Kit (ThermoFisher Scientific) in a MastercyclerPro® (Eppendorf, Framingham, MA). The cDNA (1-2 ng) was used for real time PCR (RT-PCR). RT-PCR was performed with iQ SYBR®Green Mastermix (BioRad) in a C1000 Thermal Cycler (BioRad) with the CFX Manager 3.1 (BioRad). All results were normalized to *gapdh* by using the 2-ddCT method. Primers used for RT-PCR can be found as *SI Appendix*, Supplementary Table S4.

Chromatin Immunoprecipitation (ChIP)

The Magna ChIP kit (Millipore) was used. Cells were fixed in 1% parformaldehyde for 8 minutes at room temperature. DNA was sonicated to a length of 500-700 bp at 4°C (4x10 cycles, 50% amplitude, 30s pulse, 30s rest) with sonicator Q700 (QSONICA, Newtown, CT). Antibodies (1.5 µg/µl) are listed in *SI Appendix* Supplementary Table S3.

Hydroxyproline Assay

Hydroxyproline concentration was detected in lung tissue and BALF using a Hydroxyproline Assay Kit (Sigma-Aldrich) according to the manufacturer's instructions. Briefly, homogenized lungs and BALF were hydrolyzed in concentrated hydrochloric acid for 3 h at 120°C. Hydroxyproline concentrations were measured at 560 nm and fitted on a standard curve based on the color change due to the oxidized reaction of hydroxyproline with Chloramine T and diluted 4-(dimethylamino)benzaldehyde reagent.

Histology

The lungs were filled with 500 µl of 4% formaldehyde and fixed overnight. Paraffin-embedded sections were stained according to the Masson-Goldner's Trichrome protocol. Digital images were generated with an inverted OLYMPUS IX73 microscope with a SC30/CMOS camera.

Immunohistochemistry

A Ventana Discovery Ultra (Roche, Basel, Switzerland) tissue autostainer was used for brightfield immunohistochemistry. Antigen retrieval was conducted using a Cell Conditioning Solution 1 buffer (Roche). The CD42b primary monoclonal antibody (Abcam) was incubated for 40 min at 37°C and was of rabbit origin, and accordingly was developed with a secondary goat anti-rabbit HRP-polymer antibody (Vector Laboratories, Burlingame, CA) for 20 min at 37°C. Antigen detection in brightfield slides was performed using a ChromoMap DAB Kit (Roche). Slides were counterstained with hematoxylin and mounted were imaged using a Vectra Polaris TM Quantitative Pathology Imaging System (Akoya Biosciences, Marlborough, MA).

Whole Slide Scanning

Brightfield slides were imaged using a Vectra Polaris TM Quantitative Pathology Imaging System and imported as a whole slide image in HALO (Indica Labs, Albuquerque, NM). Quantitative analysis of brightfield immunohistochemistry was done using slide images of CD42b-stained whole lungs (both lobes). For quantifying the area of the slide that contained CD42b, an algorithm termed the HALO (Indica Labs) Area Quantification (AQ) module (v2.1.11) was used and fine-tuned to quantify the immunoreactivity for the CD42b protein based on color and stain intensity. Minimum dye intensity thresholds were established using the real-time tuning field of view module to accurately detect positive immunoreactivity. This algorithm

outputted the percent of total area displaying immunoreactivity across the annotated whole slide scan in micrometers squared (μm²) across the whole lung.

Reagents

Purified histones from calf thymus (Sigma-Aldrich) were tested endotoxin-free (<0.1 EU/ml; Endotoxin Quantification Kit Pierce® LAL, ThermoFisher Scientific); rmIL-27 (R&D Systems, Minneapolis, MN); rhTGFβ1 (R&D Systems); azide-free, anti-H4 antibody (clone BWA3) was purified (QC check: SDS-PAGE) using protein A liquid chromatography as contracted antibody production (BioXCell, Lebanon, NH) to avoid contamination with SLPI (10); matched mouse isotype control IgG1k (clone MOPC-21); LDH assay kit (Pierce ThermoFisher Scientific). The entire lists of reagents and antibodies are presented as *SI Appendix* Supplementary Tables S3, S5.

References

1. G. A. Taylor *et al.*, A pathogenetic role for TNF alpha in the syndrome of cachexia, arthritis, and autoimmunity resulting from tristetraprolin (TTP) deficiency. *Immunity* **4**, 445-454 (1996).
2. L. L. Hubbard, M. N. Ballinger, C. A. Wilke, B. B. Moore, Comparison of conditioning regimens for alveolar macrophage reconstitution and innate immune function post bone marrow transplant. *Exp Lung Res* **34**, 263-275 (2008).
3. M. Bosmann *et al.*, CD11c+ alveolar macrophages are a source of IL-23 during lipopolysaccharide-induced acute lung injury. *Shock* **39**, 447-452 (2013).
4. J. Roewe *et al.*, Neuroendocrine Modulation of IL-27 in Macrophages. *Journal of immunology* **199**, 2503-2514 (2017).
5. M. Bosmann *et al.*, Interruption of macrophage-derived IL-27(p28) production by IL-10 during sepsis requires STAT3 but not SOCS3. *Journal of immunology* **193**, 5668-5677 (2014).
6. M. Bosmann *et al.*, Complement activation product C5a is a selective suppressor of TLR4-induced, but not TLR3-induced, production of IL-27(p28) from macrophages. *Journal of immunology* **188**, 5086-5093 (2012).
7. M. Bosmann *et al.*, Extracellular histones are essential effectors of C5aR- and C5L2-mediated tissue damage and inflammation in acute lung injury. *FASEB J* **27**, 5010-5021 (2013).
8. N. L. Sanders *et al.*, Neutrophil Extracellular Traps as an Exacerbating Factor in Bacterial Pneumonia. *Infect Immun* **90**, e0049121 (2022).
9. M. Bosmann *et al.*, The outcome of polymicrobial sepsis is independent of T and B cells. *Shock* **36**, 396-401 (2011).
10. J. A. Schenk *et al.*, Secretory leukocyte protease inhibitor (SLPI) might contaminate murine monoclonal antibodies after purification on protein G. *J Biotechnol* **158**, 34-35 (2012).

Supplementary Tables

Supplementary Table S1

Demographics of enrolled Idiopathic Pulmonary Fibrosis patients for sample analysis of externalized histones in BALF

	Patients
Sample Sizes	29
Sex	
Male	21/29 (72%)
Female	8/29 (28%)
Age (years)	64.3 ± 10.7
Weight (kg)	78.9 ± 15.1
Lung function tests	
FVC (l)	2.37 ± 0.7
FVC (% predicted)	65.2 ± 15.0
FEV1:FVC	0.88 ± 0.07
DLCO1 (mmol/min/kPa)	3.58 ± 1.19
DLCO (% predicted)	41.65 ± 12.2
Treatment	
Nintedanib	No
Pirfenidone	No
RVD	1/29 (3.4%)

Data are the mean (±SD). FVC: forced vital capacity, FEV1: forced expiratory volume in 1 second, DLCO1: diffusion capacity of lung for carbon monoxide, RVD: right ventricular dysfunction.

Supplementary Table S2

Lentiviral Particles (pLKO.1-puro Vector, MISSION®, Sigma-Aldrich)

Clone	Sequence (5‘-3‘)*
Smad3/shRNA1 (TRCN0000089023)	CCGG**CCCATGTTTCTGCATGGATTT**CTCGAG **AAATCCATGCAGAAACATGGG**TTTTTG
Smad3/shRNA2 (TRCN0000089024)	CCGG**GCACACAATAACTTGGACCTA**CTCGAG **TAGGTCCAAGTTATTGTGTGC**TTTTTG
Non-target (non-mammalian)/shRNA (SHC002V)	CCGG**CAACAAGATGAAGAGCACCAA**CTCAG **TTGGTGCTCTTCATCTTGTTG**TTTTTG

*The sense/antisense sequences of shRNAs are shown in bolt and loop sequences are underlined. Sequences provided by courtesy of Dr. R. Ebel (Sigma-Aldrich, Germany).

Supplementary Table S3

Antibodies

	Isotype	Clone	Manufacturer
Antibodies for Flow Cytometry			
APC anti-mouse CD4	Rat IgG2a,κ	RM4-5	BioLegend
APC anti-mouse F4/80	Rat IgG2a,κ	BM8	BioLegend
APC anti-mouse Ly6G	Rat IgG2a,κ	1A8	BioLegend
APC Isotype Ctrl	Rat IgG2a,κ	RTK2758	BioLegend
APC anti-mouse/rat IL-17A	Rat IgG2a,κ	eBio17B7	eBioscience
APC Isotype Control	Rat IgG2a,κ	eBR2a	eBioscience
FITC CD4	Rat IgG2a,κ	RM4-5	eBioscience
FITC Isotype Control	Rat IgG2a,κ	eBR2a	eBioscience
Pacific Blue anti-CD4	Rat IgG2b,κ	RM4-5	BioLegend
Pacific Blue anti-mouse/human CD11b	Rat IgG2b,κ	M1/70	BioLegend
Pacific Blue Isotype Ctrl	Rat IgG2a,κ	RTK4530	BioLegend
PE anti-mouse CD11c	Arm. Hamster IgG	N418	eBioscience
PE Isotype Control	Arm. Hamster IgG	eBio299Arm	eBioscience
eFluor450 anti-mouse CD45	Rat IgG2b,κ	30-F11	eBioscience
eFluor450 Isotype Control	Rat IgG2b,κ	eB149/10H5	eBioscience
PE anti-mouse IL-27p28	Mouse IgG2a,κ	MM-27-7B1	eBioscience
PE Isotype Control	Mouse IgG2a,κ	MOPC-173	eBioscience
PE anti-mouse pSmad2$^{(pS465/pS467)}$ / pSmad3$^{(pS423/pS425)}$	Mouse IgG1,κ	O72-670	BD
PE anti-mouse/rat/human Foxp3	Mouse IgG1,κ	150D	BioLegend
PE Isotype Ctrl	Mouse IgG1,κ	MOPC-21	BioLegend
PE F(ab')2 donkey anti-rabbit IgG	Donkey IgG	Polyclonal	eBioscience
Anti-mouse Smad3	Rabbit IgG	E.980.9	Thermo Scientific
TruStain fcX (anti-mouse CD16/32)	Rat IgG2a,λ	93	BioLegend
V450 Isotype Control	Rat IgG1,κ	R3-34	BD
V450 anti-mouse IFN-γ	Rat IgG1,κ	XMG1.2	BD
Anti-mouse Histone H3 (citrulline R2 + R8 + R17)	Rabbit IgG	Polyclonal	Abcam
AF488 anti-rabbit IgG	Goat IgG	Polyclonal	Abcam
Antibodies for Immunohistochemistry			
Anti-CD42b	Rabbit IgG	SP219	Abcam
Anti-rabbit IgG	Goat IgG	Polyclonal	Vector
Antibodies for Chromatin Immunoprecipitation			
Anti-histone H3	Rabbit IgG	D2B12	Cell Signaling
Anti-mouse Smad3	Rabbit IgG	Polyclonal	Abcam
Normal rabbit IgG		#2729	Cell Signaling

Supplementary Table S3 (continued)

Antibodies

	Isotype	Clone	Manufacturer
Blocking Antibodies (azide-free)			
Anti-Histone H4	Mouse IgG1,κ	BWA3	BioXcell (customized)
Isotype Control, LEAF™	Mouse IgG1,κ	MOPC-21	BioLegend
Anti-IL-10R	Rat IgG1	1B1.3a	Dr. M. Radsak
Isotype Control	Rat IgG1		Dr. M. Radsak
Anti-TGFβ1/2/3	Mouse IgG1	1D11	R&D Systems
Isotype Control	Mouse IgG1	11711	R&D Systems
Activating Antibodies (azide-free)			
Anti-mouse CD3ε, LEAF™	Arm. Hamster IgG	145-2C11	BioLegend
Anti-mouse CD28, LEAF™	Syrian Hamster IgG	37.51	BioLegend

Supplementary Table S4

Primer sequences

Primer	Sequence / Manufacturer
Mouse Collagen type I α2 (fo)	5′-CCAGAGTGGAACAGCGATTAC-3′, Invitrogen
Mouse Collagen type I α2 (re)	5′-GCAGGCGAGATGGCTTATTT-3′, Invitrogen
Mouse Ebi3 (fo)	5′-GGCTGAGCGAATCATCAA-3′, Invitrogen
Mouse Ebi3 (re)	5′-GAGAGAGAAGATGTCCGGGAA-3′, Invitrogen
Mouse Ebi3_prom (fo)	5′-CAGGTTCCCTGTGTGAGTCC-3′, Invitrogen
Mouse Ebi3_prom (re)	5′-GCTCTGTGGCTCTGTTCCTT-3′, Invitrogen
Mouse FSP-1 (fo)	5’-TTCCAGAAGGTGATGAG-3’, Invitrogen
Mouse FSP-1 (re)	5’-TCATGGCAATGCAGGACAGGAAGA-3’, Invitrogen
Mouse Gapdh (fo)	5′-TACCCCCAATGTGTCCGTCGTG-3′, Invitrogen
Mouse Gapdh (re)	5′-CCTTCAGTGGGCCCTCAGATGC-3′, Invitrogen
Mouse IL-27(p28) (fo)	5’-GGCCATGAGGCTGGATCTC-3’, Invitrogen
Mouse IL-27(p28) (re)	5’-AACATTTGAATCCTGCAGCCA-3’, Invitrogen
Mouse IL-27(p28)_prom (fo)	5′-CCCTCTGGGAAGGGAAATTA-3′, Invitrogen
Mouse IL-27(p28)_prom (re)	5′-CCTCTGTGTGCAGCCATCT-3′, Invitrogen
Mouse Slug (fo)	5′-CGCTCCTTCCTGGTCAAGA-3′, Invitrogen
Mouse Slug (re)	5′-AGGTATAGGGTAACTTTCATAGAGATA-3′, Invitrogen
Mouse Smad3 (fo)	5′-GGATGGTCGGCTGCAGGTGTCC-3′, Invitrogen
Mouse Smad3 (re)	5′-TGTTGAAGGCAAACTCACAGAGC-3′, Invitrogen
Mouse Snail (fo)	5′-GTGCCCACCTCCAAACCC-3′, Invitrogen
Mouse Snail (re)	5′-AAGGACATGCGGGAGAAGG-3′, Invitrogen
Mouse TTP (fo)	5′-TTATGTTCCAAAGTCCTCCGA-3′, Invitrogen
Mouse TTP (re)	5′-CCATGGATCTCTCTGCCATC-3′, Invitrogen
Mouse Vimentin (fo)	5’-CGGAAAGTGGAATCCTTGCA-3’, Invitrogen
Mouse Vimentin (re)	5’-CACATCGATCTGGACATGCTGT-3’, Invitrogen
Mouse Zeb2 (fo)	5’-GGCGCAAACAAGCCAATCCCA -3’, Invitrogen
Mouse Zeb2 (re)	5’-TTCACTGGACCATCTACAGAGGCTT -3’, Invitrogen
Mouse α-SMA (fo)	5’-CGGGCTTTGCTGGTGATG-3’, Invitrogen
Mouse α-SMA (re)	5’-CCCTCGATGGATGGGAAA-3’, Invitrogen

Supplementary Table S5

Reagents

Pattern Recognition Receptor Agonists	Concentration*	Manufacturer
LPS (E.coli 0111:B4)	100 ng/ml	Sigma Aldrich
Zymosan	10 µg/ml	InvivoGen
LTA	10 µg/ml	InvivoGen
Poly(I:C)	1 µg/ml	InvivoGen
5' ppp-dsRNA	200 ng/ml	InvivoGen
Cytokines		
rhTGFβ1	10 ng/ml	PeproTech
rmIFN-γ	10 ng/ml	PeproTech
rmIL-27	10 ng/ml	R&D Systems
rmIL-4	10 ng/ml	PeproTech
Proteins		
Human Thrombin (Endotoxin: <1.0 EU/1 µg)	100 ng/ml	R&D Systems
Calf Thymus Histones (Endotoxin: <0.1 EU/ml)		Sigma Aldrich
Citrullinated Calf Thymus Histones		Cayman Chemical
Recombinant Human Citrullinated Histone H3	50µg/mL	Cayman Chemical
Recombinant Human Human H2A	50µg/mL	The Histone Source[§]
Recombinant Human Human H2B	50µg/mL	The Histone Source
Recombinant Human Human H3	50µg/mL	The Histone Source
Recombinant Human Human H4	50µg/mL	The Histone Source
Small Molecule Inhibitors		
SB431542	1-20 µM	Tocris
BIRB796	50 nM	Calbiochem
PH-797804	10 nM	Selleckchem
SB203580	10 µM	Jena Bioscience
Kits		
LDH assay	-	ThermoFisher
Hydroxyproline Assay		Sigma Aldrich

* If not specified otherwise in figure legends. [§] The Histone Source at Colorado State University, Fort Collins, CO

Supplementary Figures

SI Appendix, Fig. S1

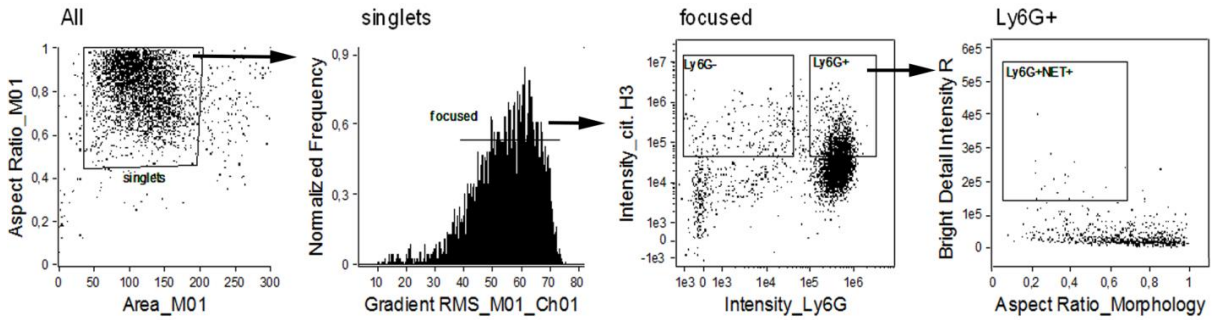

Fig. S1. Imaging flow cytometry gating. Immune cells in BALF of C57BL/6J mice after bleomycin were stained with antibodies for citrullinated histone H3 (citH3) and Ly6G. Singlets were gated for these two markers and analyzed for a low aspect ratio (morphology mask) and high bright detail intensity in the citH3 channel.

SI Appendix, Fig. S2

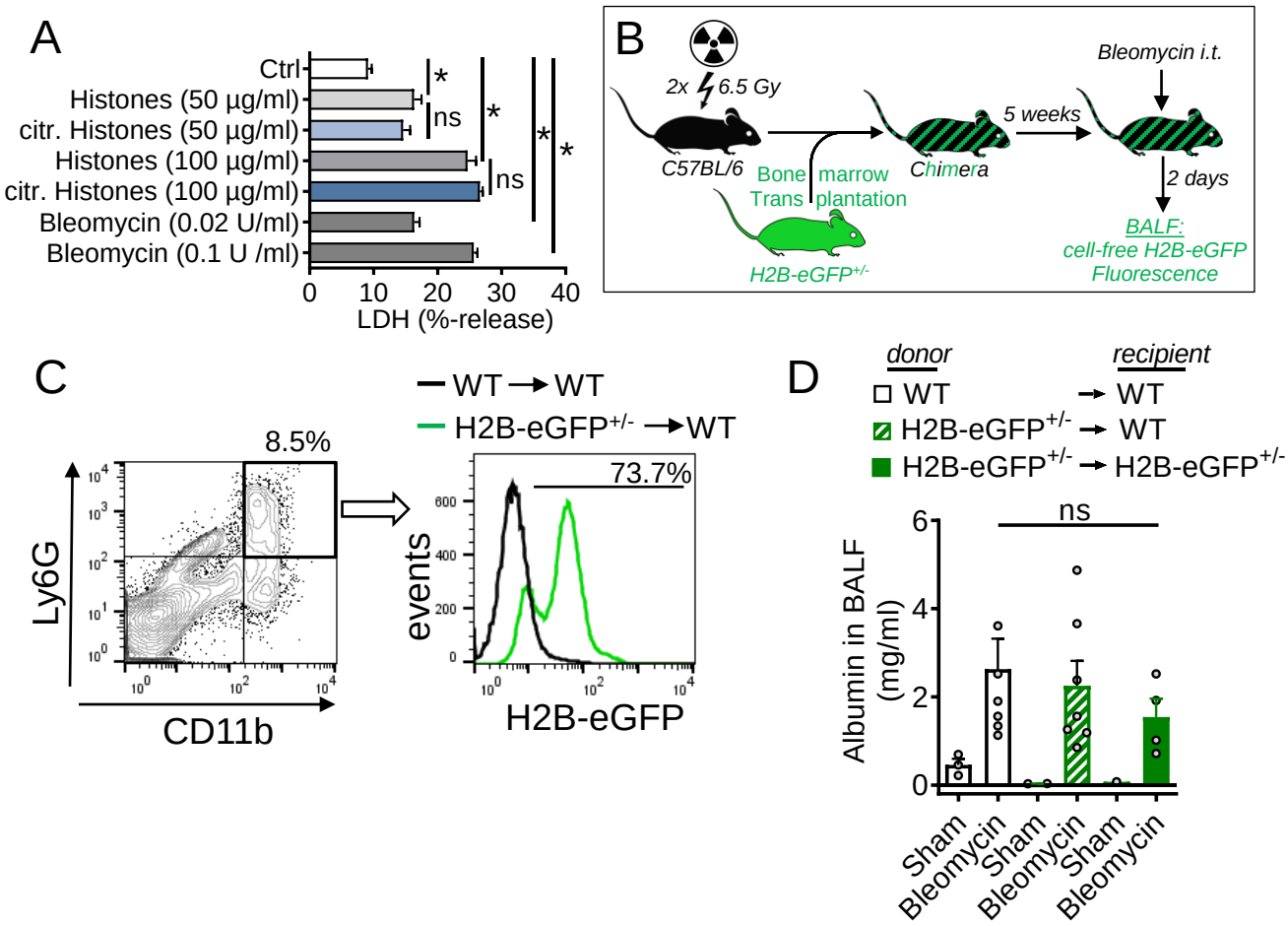

Fig. S2. Studies on the roles of extracellular histones. (*A*) Lactate dehydrogenase (LDH) release assay of supernatants from MLE-12 lung epithelial cells for the evaluation of cytotoxicity mediated by incubation with purified histones, citrullinated histones and bleomycin, 24h. (*B*) Schematic of the experimental design to assess the fractions of externalized histones released by hematopoeitic cells and lung stromal cells. C57BL/6J (WT) recipient mice were lethally irradiated (2x6.5 Gy) and injected with bone marrow cells from reporter H2B-eGFP donor mice. After 5 weeks, the chimeric mice were subjected to bleomycin-induced lung injury and fluorescence in cell-free BALF was detected following another 2 days. (*C*) Engraftment at 5 weeks after transplantation in chimeric mice (n=3/group) as compared to WT→WT controls as analyzed by eGFP fluorescence in bone marrow with gating on $Ly6G^+CD11b^+$ neutrophils. (*D*) Chimeric mice and control groups were generated as described above and subjected to bleomycin-induced lung injury. Sham mice received 40 µl NaCl 0.9% i.t. The severity of injury to the alveolar/capillary lung barrier was assessed by detection of albumin in BALF after 2 days; one-way ANOVA; *P<0.05; ns: not significant.

SI Appendix, Fig. S3

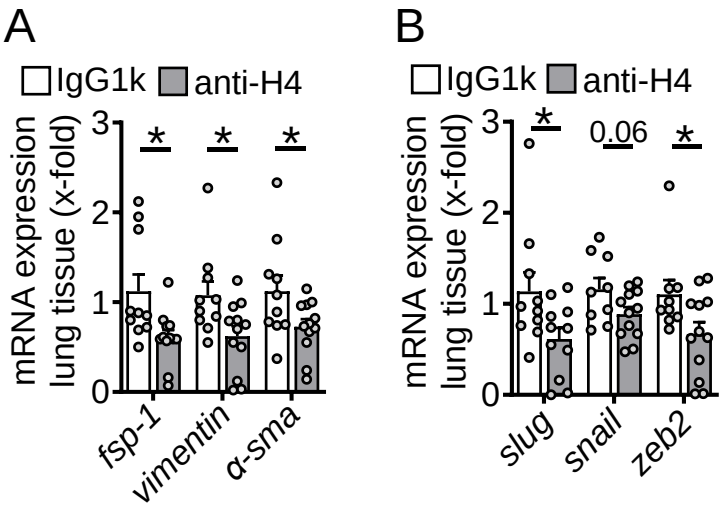

Fig. S3. Studies on markers of epithelial-to-mesenchymal transition. C57BL/6J mice received bleomycin (1 U/kg body weight i.t.) along with antibody neutralization of histones H2A/H4 or control IgG1k antibodies. Lungs were collected and homogenized after 4 weeks. (*A*) Gene expression of *fsp-1*, *vimentin* and *α-sma*, RT-PCR. (*B*) Gene expression of the transcription factors, *slug*, *snail*, and *zeb2,* RT-PCR. Numbers of mice in frames *A*-B are indicated by circles and mice were from the same experiments as for Fig. 2*B-F*. One-way ANOVA; *P<0.05.

SI Appendix, Fig. S4

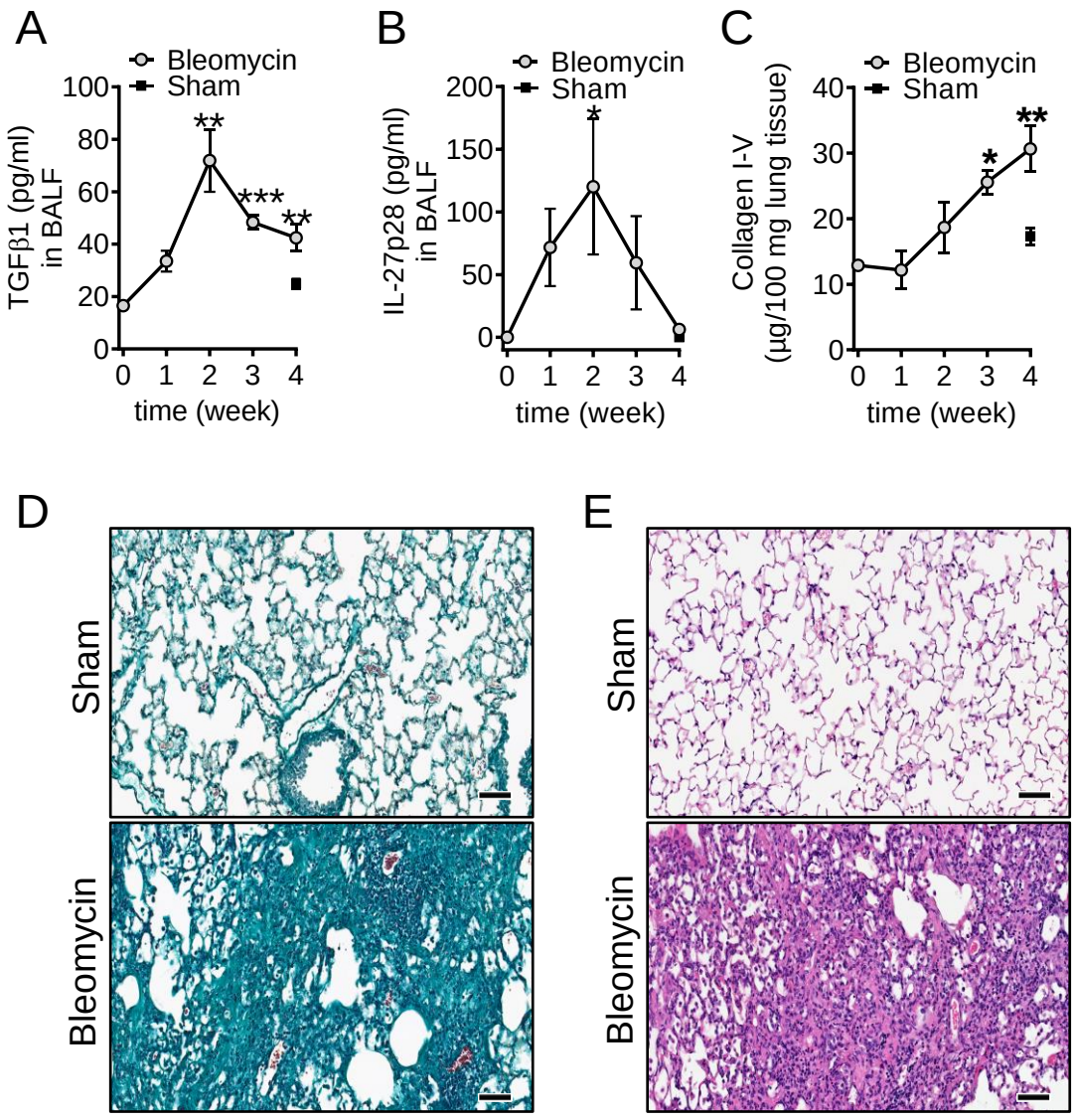

Fig. S4. Characterization of bleomycin-induced pulmonary fibrosis. C57BL/6J mice (8 week old males, n≥3 mice/group) received bleomycin (1 U/kg body weight i.t.) and were analyzed on week 0-4. Sham mice received 40 µl NaCl 0.9% i.t and were analyzed after 4 weeks. (*A*) Concentrations of TGFβ1 in BALF, ELISA. (*B*) Concentrations of IL-27p28 in BALF, ELISA. (*C*) SIRCOL assay of collagen I-V protein in homogenated lungs. (*D*) Masson-Goldner's trichrome staining of lungs after 4 weeks. (*E*) Hematoxylin and Eosin staining of lungs after 4 weeks, scale bar: 50 µm. One-way ANOVA; *P<0.05, **P<0.01, ***P<0.001.

SI Appendix, Fig. S5

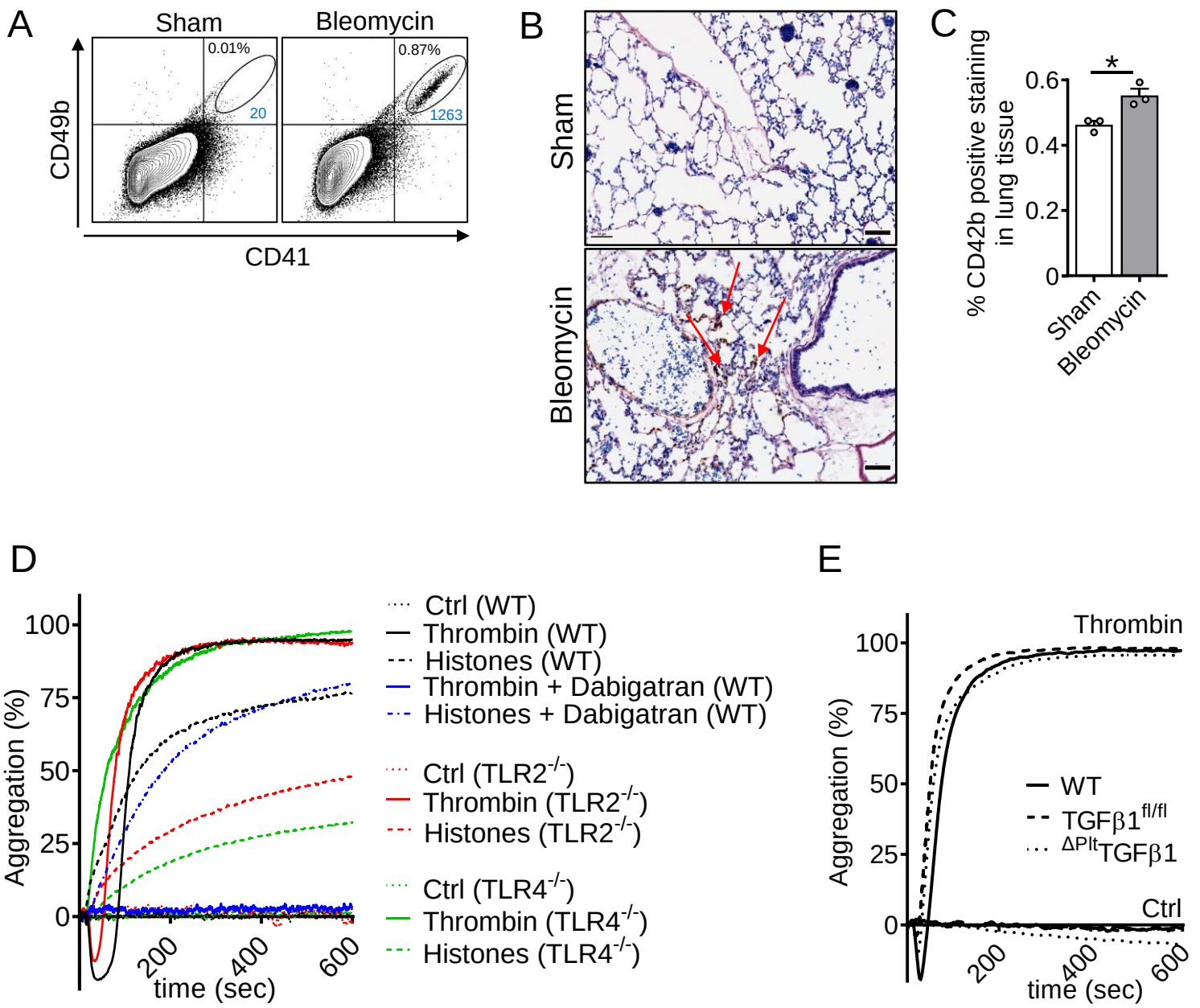

Fig. S5. Studies of platelets. (*A*) $CD41^{+}CD49b^{+}$ platelets in BALF of C57BL/6J mice after bleomycin-induced lung injury as compared to sham treatment with saline i.t., 12 h, flow cytometry. (*B*) $CD42b^{+}$ platelets (red arrows) in lung sections of C57BL/6J mice after bleomycin-induced lung injury as compared to sham treatment with saline i.t., 12 h, brightfield immunohistochemistry, n=3/group. (*C*) Quantification of $CD42b^{+}$ staining from scanned whole slides of mice as in frame *B*. (*D*) Aggregometry of washed platelets from C57BL/6J (WT) mice, $TLR2^{-/-}$ mice and $TLR4^{-/-}$ mice activated with purified histones (50 µg/ml), thrombin (100 ng/ml) or left as unstimulated controls (Ctrl). The thrombin effect was antagonized by the direct thrombin inhibitor, dabigatran (500 nM). (*E*) Superimposable curves in platelet aggregometry of washed platelets from mice with platelet-specific deletion of TGFβ ($^{\Delta Plt}$TGFβ1) and $TGFβ1^{fl/fl}$ controls after addition of thrombin (100 ng/ml). Frames A, D-E show representatives of two independent experiments.

SI Appendix, Fig. S6

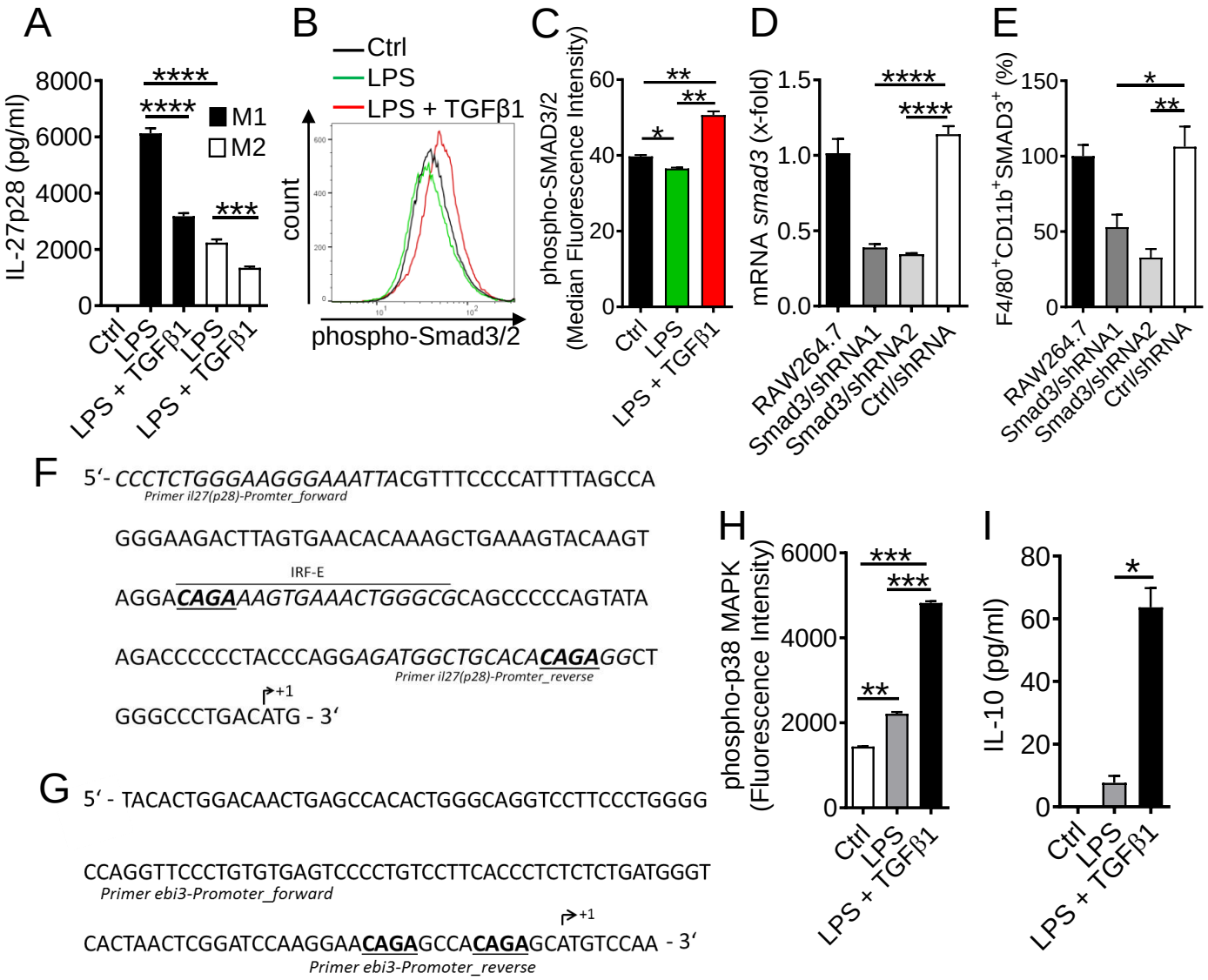

Fig. S6. Data on IL-27 and signaling in macrophages. (*A*) Release of IL-27p28 from M1 polarized (IFNγ, 10 ng/ml) or M2 polarized (IL-4, 10 ng/ml) BMDM (C57BL/6J) macrophages in dependency of incubation with LPS (100 ng/ml) ± TGFβ1 (10 ng/ml), 24 h, ELISA. (*B*) Flow cytometry of phosphorylated SMAD3/SMAD2 (Ser^{465}/Ser^{467}, Ser^{423}/Ser^{425}) in $F4/80^+CD11b^+$ macrophages (BMDM) following incubation with LPS and TGFβ1 for 30 minutes. Ctrl denotes unstimulated control macrophages. (*C*) Flow cytometry with mean fluorescence intensities of phosphorylated SMAD3/SMAD2 in $F4/80^+CD11b^+$ macrophages (BMDM), 30 min. (*D*) Lentiviral knock-down of *smad3* mRNA in RAW264.7 macrophages by stable transduction of 2 independent shRNAs (shRNA1, shRNA2) for SMAD3. RAW264.7 denotes untransduced cells and Ctrl/shRNA denotes non-target control shRNA, RT-PCR. (*E*) Frequencies of $F4/80^+CD11b^+SMAD3^+$ RAW264.7 macrophages with shRNAs as described in *D*. Total SMAD3 was detected by indirect staining with rabbit anti-mouse SMAD3 followed by donkey anti-rabbit IgG-PE as secondary antibody before flow cytometry. (*F*) Sequence of the mouse *il-27p28* promoter region. Putative *smad3* binding sites (CAGA boxes) are shown in bolt and underlined. Transcription start sites (→+1) and primers used for ChIP assays are indicated. (*G*) Sequence of the mouse *ebi3* promoter. Putative *smad3* binding sites are shown in bolt and underlined. Transcription start sites (→+1) and primers used for ChIP assays are indicated. (*H*) Phosphorylated p38 MAPK (Thr^{180}/Tyr^{182}) in BMDM (C57BL/6J) in response to LPS ± TGFβ1, 1 h. (*I*) IL-10 concentrations in supernatants of BMDM (C57BL/6J), 9 h, ELISA. Data in frames *A-E* and *H*, *I* are representative of 2-4 independent experiments; Student's t-test; *P<0.05, **P<0.01, ***P<0.001, ****P<0.0001.

SI Appendix, Fig. S7

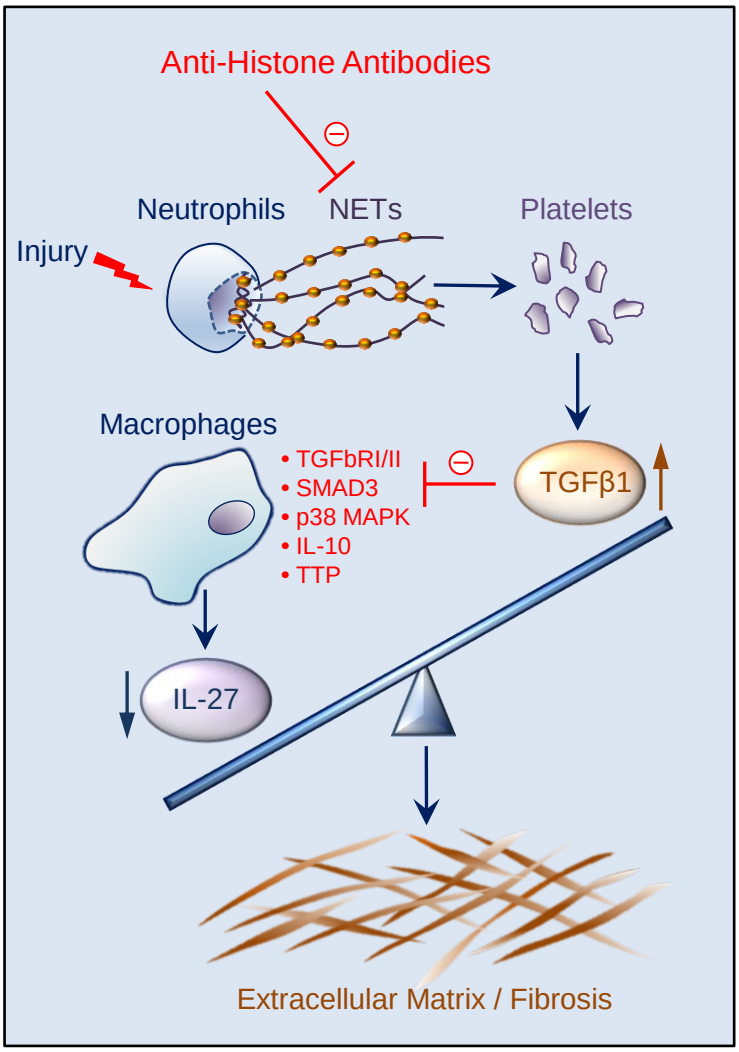

Fig. S7. Schematic illustration of the proposed inflammatory pathways during pulmonary fibrosis. Tissue injury and inflammation trigger the generation of NETs with externalized histones. Activated platelets release TGFβ1, which binds to the TGFbRI/TGFbRII receptor complex on macrophages. TGFβ1 orchestrates multiple pathways such as SMAD3, p38 MAPK, IL-10 and TTP for suppression of IL-27 from macrophages. Hence, a critical balance of platelet-derived TGFβ1 and myeloid-derived, anti-fibrotic IL-27 is skewed towards profibrotic conditions with accelerated ECM deposition. The adverse biological activities of NETs and externalized histones can be interrupted by neutralizing anti-histone antibodies.